Formation of High Aspect Ratio GaAs Nanostructures with Metal-Assisted Chemical Etching

Matt DeJarld,[†] Jae Cheol Shin,[†] Winston Chern,[†] Debashis Chanda,[‡] Karthik Balasundaram,[†] John A. Rogers,[‡,†] and Xiuling Li*,[†,‡,§]

[†]Department of Electrical and Computer Engineering, [‡]Department of Materials Science and Engineering, and [§]Micro and Nanotechnology Laboratory, University of Illinois, Urbana, Illinois 61801, United States

S Supporting Information

ABSTRACT: Periodic high aspect ratio GaAs nanopillars with widths in the range of $500-1000$ nm are produced by metal-assisted chemical etching (MacEtch) using n-type (100) GaAs substrates and Au catalyst films patterned with soft lithography. Depending on the etchant concentration and etching temperature, GaAs nanowires with either vertical or undulating sidewalls are formed with an etch rate of $1-2$ μm/min. The realization of high aspect ratio III−V nanostructure arrays by wet etching can potentially transform the fabrication of a variety of optoelectronic device structures including distributed Bragg reflector (DBR) and distributed feedback (DFB) semiconductor lasers, where the surface grating is currently fabricated by dry etching.

KEYWORDS: Nanowire, nanopillar, high aspect ratio, GaAs, MacEtch, metal-assisted chemical etching
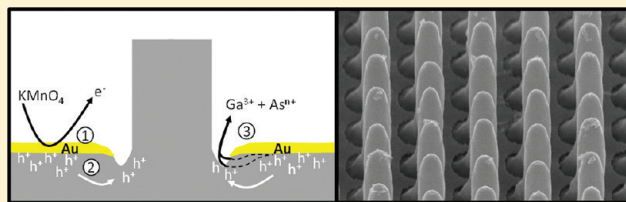
High aspect ratio semiconductor nanostructures are becoming more prevalent in many applications including solar cells, light emitting diodes (LEDs), field effect transistors (FETs), thermoelectric devices, and sensing.[1−5] These nanostructures can be formed from either the bottom up by growth or the top-down by etching. For top-down methods, one of the most used methods is reactive ion etching of a patterned substrate.[6] However, this can result in extensive damage to the crystal structure and surface morphology because of the high-energy ions involved. For silicon, such surface damage can be repaired by thermal annealing. However, for compound semiconductors, such as GaAs, thermal repair is not completely effective mainly because of the difficulty of maintaining stoichiometry.[7,8] One top-down etching method, which is becoming increasingly more favorable, is metal-assisted chemical etching (MacEtch), a simple directional wet etching method.[9]

MacEtch, first reported by Li and Bohn for silicon (Si),[10] offers a wet etching method for semiconductors that can be anisotropic, assisted by a metal catalyst. The catalyst can be patterned metal films (Ag, Au, Pt, Pd, etc.) or metal nanoparticles (e.g., Ag) formed by galvanic displacement from a solution that contains the metal salt (e.g., $AgNO_3$).[11,12] The latter results in less controlled spatial ordering and diameter distribution due to the random networks of metal nanoparticles.[13] For the former, a $20-30$ nm layer of gold or platinum can be patterned using a variety of different methods, including superionic solid-state stamping,[14] e-beam lithography,[15,16] polystyrene spheres,[17] and metal deposition masks.[18] The metal-coated Si sample is submerged into a solution of HF and H_2O_2 and a diluting agent, such as ethanol.[14] The metal acts as a local cathode catalyzing the reduction of the oxidant H_2O_2 to generate free holes at the metal−Si interface and

oxidizes Si, which reacts with the solution to form H_2SiF_6.[10] The ratio of these reactants can greatly affect the morphology and topography of the produced nanostructures.[14,15] Because it occurs near room temperature, MacEtch should not introduce metal contamination, in contrast to bottom-up high-temperature metal-catalyzed nanowire growth. Because it is a wet etch process, MacEtch avoids ion-induced surface damages typically seen in dry etch processes. This is crucial to III−V nanostructures for optoelectronic applications.

However, MacEtch of III−V materials to produce periodic nanostructures, especially in high aspect ratios, has hardly been explored. Previously, small microbump arrays of InP have been formed using MacEtch coupled with UV photoirradiation, over an extended period of time with a large ($\sim$40 μm) pattern.[18] MacEtch of GaAs has been able to produce sporadic minor crevices[19,20] and protrusions[20] by using Cu, Ag, and Pd as the metal catalyst[19,20] and hydrogen peroxide (H_2O_2) as the oxidizing agent. Regardless of the type of the semiconductor, the ideal MacEtch solution needs to be inert without the presence of metal. Although H_2O_2 has been proven to be a suitable MacEtch agent for silicon, it has been shown to etch (100) GaAs in either acidic or base solution without the presence of metal catalyst.[19−21] The main challenge of MacEtch of III−V is to find the appropriate etching condition resulting in the highest differential etch rate for the III−V semiconductors with and without metal present. Oxidizing agents with weaker potentials (e.g., $KMnO_4$) are required to prevent nonmetal-catalyzed
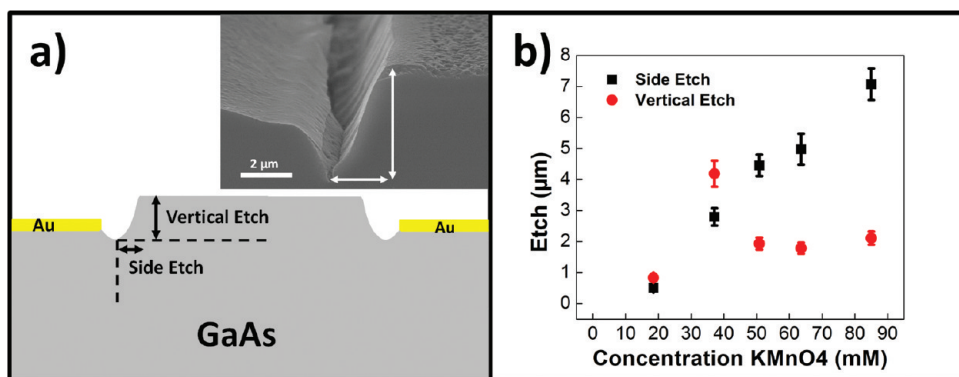
Figure 1. Effect of oxidant concentration on vertical and side etch of GaAs using a $300 \times 300\ \mu m^2$ large square Au mesh pattern that was etched in a solution of $KMnO_4$ and HF for 3 min. (a) Schematic illustration of a typical etched profile defined by vertical and side etch at the pattern edges. Inset shows a SEM image of such profile. (b) Plot of vertical and size etch depth as a function of $KMnO_4$ concentration.

etching, while maintaining a reasonable etch rate in the presence of metal.

In this paper, we investigate the etching characteristics of n-type GaAs wafers patterned by Au using soft lithography with $KMnO_4$ as the oxidizing agent in acidic (H_2SO_4 or HF) solutions as a function of solution concentration and temperature. We demonstrate that ordered arrays of high aspect ratio GaAs nanostructures can be formed using Au-MacEtch.

Epi-ready Si-doped (100) GaAs substrates acquired from AXT, Inc. with a doping concentration of $1-4 \times 10^{18}\ cm^{-3}$ were used for MacEtch. Potassium permanganate ($KMnO_4$), an oxidizing agent that has an oxidation potential lower than that of H_2O_2 (see Table 1, Supporting Information), was mixed with deionized water (DI) and either sulfuric acid (H_2SO_4) or hydrofluoric acid (HF). The overall etching of GaAs using $KMnO_4$ can be described by the following chemical reaction: $GaAs + MnO_4^- + H^+ \rightarrow Ga^{3+} + As^{n+} + Mn^{2+} + H_2O$, with n equal to 3 or 5. Several possible products of the etching reaction with mass and charge balanced are listed in the Supporting Information. The etching was carried out at either room temperature or 30−45 °C for a period of 3−5 min, as will be indicated. No stirring was done during etching.

Nanoscale Au mesh patterns, with hole size ranging between 500 and 1000 nm, were prepared using a soft lithography method.[22] First, a layer of SiN_x was deposited on top of the GaAs, followed by a spin-coated layer of SU8. Using a poly-(methyl methacrylate) (PMMA) stamp, the pattern was imprinted onto the SU8. Next the depressed SU8 was removed using an oxygen plasma etch. The sample was then subject to a CHF_4 etch to remove the exposed SiN_x. Following this step, a 20 nm layer of Au was evaporated on the GaAs surface. The remaining SiN_x and SU8 were removed with sonication in a diluted HF solution. Also tested were micrometer square patterns of $300 \times 300\ \mu m^2$ separated by 125 μm wide strips of gold formed with standard optical lithography using AZ5214 photoresist. SEM images were obtained using a Hitachi 4800 microscope and photoluminescence (PL) spectra were measured using a Renishaw micro-PL system with a 633 nm pump laser and a CCD detector at room temperature.

As mentioned earlier, MacEtch begins when holes (h^+) are generated from the oxidant on the metal surface and then diffuse to the semiconductor. The holes (h^+) can then subsequently be consumed by oxidizing the semiconductor directly underneath the metal to form soluble product in the acidic solution. This leads to vertical etching. Alternatively, the holes can diffuse outside of the metal−semiconductor interface to areas around the metal to induce lateral etching. The aspect ratio of a produced structure is inherently related to the proportion of vertical to lateral etching, which is the essence of the MacEtch mechanism. Processing factors that affect the dynamics of MacEtch can be classified into three categories: (1) semiconductor type and doping; (2) metal type, feature size, and density; and (3) solution components, concentration, temperature, and local concentration fluctuation. The focus of this study is on the third factor that limits aspect ratios, i.e., the solution. In particular, we explore the effect of oxidizing agent potential and concentration, chemical end product, accessibility to solution as a result of metal pattern size, and temperature on the etching dynamics and aspect ratio of GaAs nanostructures produced by this method.

In order to produce high aspect ratio structures, lateral etching must be suppressed. Figure 1 presents the effect of the oxidant concentration on the etching direction by using large size Au mesh patterns ($300 \times 300\ \mu m^2$ separated by 125 μm). For metal patterns of such large size, etching takes place mostly around the edges of the metal pattern, while areas under the middle of the metal pads have limited access to solution which prevents product removal. Accumulated holes from the metal covered areas tend to diffuse laterally and side etch occurs. Figure 1a is a schematic illustration of the typical topography produced from patterns of this size as well as a SEM image showing the trenched profiles. The trenched etching structures are measured on two parameters: vertical etch depth and side (lateral) etch length.

Figure 1b shows the effect of the concentration of oxidizing agent $KMnO_4$ on the vertical vs side etch rate. The vertical and side etching depths are plotted using the average depth measured over multiple squares on the same sample, and the standard deviation is plotted as the error bar. It can be seen that as $KMnO_4$ concentration increases, the vertical etch depth peaks at a concentration of 37 mM and then drops to a relatively stable value. This concentration also exhibits the best aspect ratio (vertical/side etch depth). Further increase in concentration causes the side etch to surpass the vertical etch rate, as more holes are produced at higher concentrations of $KMnO_4$. In order to form completely ordered structures with vertical sidewalls, the dissolution step of MacEtch reaction needs to be uniform across the patterned area.
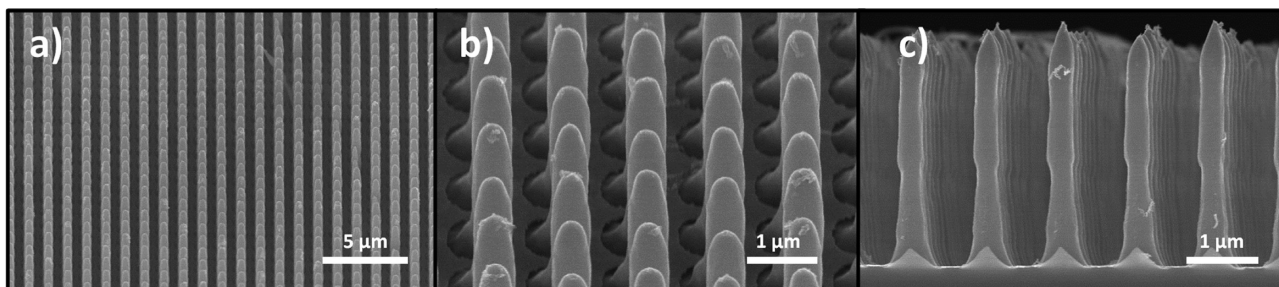
Figure 2. SEM images of high aspect ratio GaAs nanopillars produced from a 600 nm wide square Au mesh pattern in H_2SO_4 and $KMnO_4$ solution at 40−45 °C. (a) 30° tilted view at low magnification, (b) 30° tilted view at high magnification, (c) cross-sectional showing the highly vertical nanopillar array.

Note that patterns of hundreds of micrometers had to be used to evaluate side etch. If the side etch is larger than the radius of the nanostructure's lateral dimension, it will result in polishing with no discernible structure formation. Due to the difference in the supply of holes (h^+) for oxidation and end product removal rate, the optimum etching recipe varies as a function of metal pattern size and connectivity. MacEtch of GaAs at nanoscale dimensions is found to be very sensitive to all etching parameters. For Au mesh patterns at submicrometer scales, most combinations of oxidant to acid ratio, dilution, and temperature resulted in either no etching or polishing from overetching. A suitable etching condition is determined by calibrating between the two extremes.

Shown in Figure 2 is an array of highly vertical GaAs nanopillars produced from an Au mesh pattern with 600 nm diameter openings in a solution of H_2SO_4 over-saturated with $KMnO_4$ at slightly elevated temperature for 5 min. The nanopillars formed are ∼3.5 μm tall and ∼600 nm in width. The Au mesh pattern descends to the bottom of the pillar structure and can be seen clearly in Figure 2b, just as is the case for Si MacEtch. The tips of the nanopillars appear to be tapered, probably resulting from lateral etching at the initial stage. Slight nonuniformity in the pillar width can be seen in the cross-sectional SEM image near half height of the wire. However, the position of the narrow neck appears to be synchronized for all pillars, implying that this is due to local etchant concentration fluctuations in the solution. Nevertheless, large area periodic arrays of ordered GaAs nanopillars are produced using MacEtch in a matter of minutes. Importantly, the solution has to be kept between 40 and 45 °C during etching. Note that using the same solution, no etching was observed at room temperature, while at temperatures higher than 45 °C, the Au pattern delaminates from the substrate surface.

Interestingly, at a slightly lower temperature range of 30−35 °C, a metal mesh pattern of similar dimensions using the same solution etched for the same period of time acts as an etching mask for GaAs. Etching is promoted in the areas without Au coverage, yielding a GaAs grid structure with craters that have an initially sloped sidewall but a flat bottom with a depth of approximately 0.5 μm, as shown in Figure 3.

We hypothesize that at this temperature, the etching reaction is dissolution limited. The rate-determining step is the removal of the oxidized Ga^{3+} and As^{n+} ($n = 3^+$ or 5^+) into solution (e.g., $Ga_2(SO_4)_3$ and $HAsO_2$). As a result, the holes (h^+) generated at the gold surface are not consumed in time and instead diffuse laterally to promote etching of the bare GaAs. Similar reverse MacEtch was reported for InP under photoirradiation.[18] In that case, the above bandgap photons generate electrons and holes in the bare InP area; the electrons then diffuse and recombine with the holes generated from metal-catalyzed oxidant reduction in the metal-covered area, causing holes to accumulate and etch the bare InP region.

These results indicate that etching temperature can affect the dynamics of carrier diffusion, oxidation, and product removal, all of which are important to the spatial profile of GaAs structures generated by patterned MacEtch.

Furthermore, striking zigzagging high aspect ratio nanowires are formed by MacEtch using a solution of $KMnO_4$ and HF in a glass beaker at room temperature. Shown in Figure 4 is an array of wires with zigzagging sidewalls formed from a 1.0 μm diameter mesh pattern etched using 55.7 mM of $KMnO_4$ in HF for 5 min. From the zoomed in side image (Figure 4b), it can be seen that the zigzag pattern is synchronized horizontally. Also, the twisting direction is close to ⟨111⟩ crystal orientation based on measured angles from the SEM images. It is known that MacEtch can
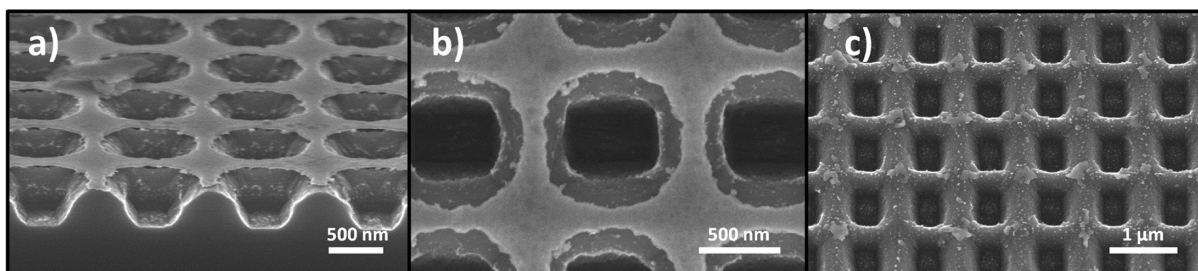
Figure 3. SEM images of periodic indentations created by inverse MacEtch using the same Au pattern as in Figure 2 but Au acts as a mask in H_2SO_4 and $KMnO_4$ solution at 30−35 °C. (a) Tilted and (b) top views with Au still on top of the surface, and (c) top view from an area with most of the Au peeled off.
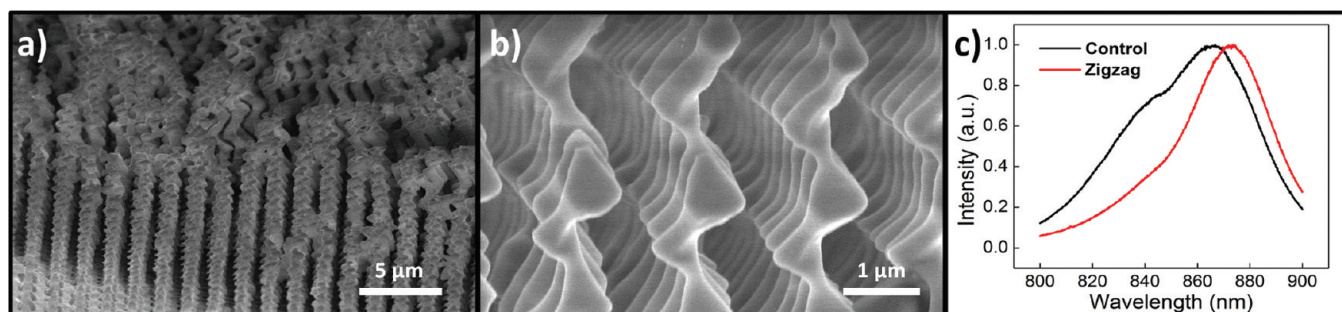
Figure 4. Cross-sectional view SEM images of an array of zigzagging GaAs nanowires at (a) low and (b) high magnifications, formed from MacEtch using 1 μm wide square Au mesh pattern at 55.7 mM concentration of KMnO4 in HF solution carried out in a glass beaker. The tips of the nanowires in (a) are clumped together due to surface tension when the wires are tall. (c) Room temperature PL spectra taken from the zigzagged GaAs nanowires, along with an unetched area of the GaAs substrate. The peaks are at 870 and 880 nm, respectively.

propagate along different orientations with different etchant concentration, and high HF/oxidant ratio prefers etching along ⟨111⟩ directions for Si (100) substrate.[14] We believe concentration modulation is the reason for the observed zigzagging GaAs nanowires which twist left and right from one ⟨111⟩ orientation to another, joined by the straight ⟨100⟩ segments.

It has been reported that zigzag Si nanowires were formed using (111) Si wafers through MacEtch with solution-based Ag catalyst AgNO₃.[13] Notably, an intentionally scratched rough surface led to zigzag, while polished smooth surface yielded straight wires. In another report,[23] an initial porous silicon layer was deemed important for the formation of zigzag Si nanowires for Si(100) surface using patterned Au mesh as catalyst at an elevated temperature (60 °C). The porous layer acted as a barrier to deter diffusion of MacEtch reactants in the unstirred solution, creating high and low concentrations as reactants were consumed because there was a delay in replenishing them. The authors also attributed the zigzag morphology to the concentration variations.

In our case, intentional surface roughening did not produce zigzagging structures. However, carrying out the reaction in a glass container with HF acid was necessary, implying that the borosilicate glass container participated in the etching reaction. We hypothesize that the glass surrounding the solution is constantly turning HF into H_2O, which creates a concentration gradient that drives the diffusion of HF directly above the semiconductor wafer piece toward the container walls. In competition with the outward diffusion, HF is consumed from reacting with GaAs during MacEtch, causing the diffusion to shift back toward the wafer piece to rebalance the concentration. The constant modulation of flux during etching creates a periodic concentration variation similar to the zigzagging Si nanowire etching condition reported by Kim et al.[23] Although the borosilicate container reaction replicated an extreme case of concentration variations during etching, the resulting nanowire morphology clearly demonstrates the susceptibility of GaAs MacEtch to local solution fluctuations.

Figure 4c shows the PL spectrum taken from the zigzagged nanowires along with an unetched area on the same sample. A distinct shift toward longer wavelength by ∼9 nm relative to bulk GaAs is observed for the zigzagged nanowires, and smaller (∼ 3 nm) red shift (not shown) has also been observed for other nanowire structures formed. The red shift might be from some shallow surface states which become more prevalent for nanowires due to the increased surface area. Further investigation is needed to elucidate the origin of this shift.

To summarize, Figure 5 shows schematic illustrations of the formation mechanism of the GaAs nanostructures reported here. Three processes labeled 1, 2, and 3 correspond to the three steps in MacEtch: hole formation, hole diffusion, and semiconductor oxidation and removal. Figure 5a corresponds to MacEtch involving H_2SO_4 at high temperature (40−45 °C), where the holes are removed as soon as they reach the boundary of Au, GaAs, and solution. This scenario results in high aspect ratio vertical wall nanopillars, as shown in Figure 2. Figure 5b represents MacEtch involving H_2SO_4 at mid-temperature range (30−35 °C), where there is an excess amount of holes accumulates in the bare GaAs area because the lower temperature severely reduces the rate of step 3. This mechanism leads to reverse MacEtch, as shown in Figure 3, where metal acts as a mask. Figure 5c illustrates the scenario of Figure 4, where MacEtch involves local concentration fluctuation induced by consumption and rebalance of HF/KMnO₄ by the boroslicate glass. The concentration modulation forces the nanowires to exhibit a zigzag morphology.

In conclusion, by adapting the MacEtch solution to GaAs, we have demonstrated that MacEtch, a wet but directional etching method, can produce high aspect ratio semiconductor nanoscale structures beyond just silicon. In contrast to MacEtch of Si, the process window for GaAs is more sensitive to the rate of oxidation with and without the Au catalyst and rate of dissolution for etching product removal as well as changes in the local concentration during etching. By exploiting the effect of etching parameters, different nanostructures can be formed for a variety of applications, including DBR or DFB lasers, photonic crystals, LEDs with periodic roughening surfaces, and solar cells with light trapping nanostructures. Since the etching takes place at near room temperature, no metal contaminants should be incorporated in the core of the nanopillars, and surface contamination can be removed. Because there is no high energy ions involved, as in the case of dry etching, surface damage should not be a concern. Because the aspect ratio is essentially limited by etching time, as long as unassisted etching mechanism such as side etching can be suppressed, extremely high aspect ratio vertical structures can be generated. Although only n-type GaAs is demonstrated here, with further research it should be possible for MacEtch to work for III−V materials of various doping types and levels as well as heterostructures. The realization of high aspect ratio III−V nanostructure arrays by MacEtch can potentially transform the fabrication of a variety of optoelectronic device structures including DBR and DFB semiconductor lasers,
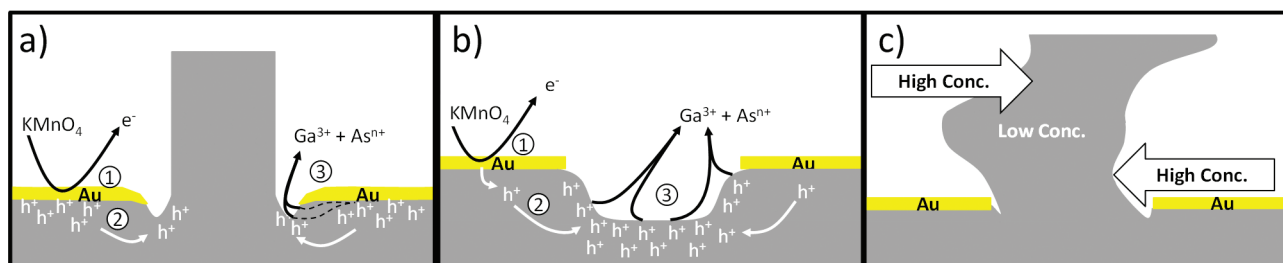
Figure 5. Schematic illustrations (a–c) of the formation mechanism of morphologies observed in Figures 2–4, respectively. The etching process involves the competition of three steps: (1) hole (h^+) generation from KMnO4 catalyzed by Au surface; (2) hole (h^+) diffusion; and (3) oxidation and removal of etching products (Ga^{3+} and As^{n+}, where $n = 3$ or 5). See text for details.

where surface grating is currently fabricated by dry etching. It also brings affordability and possibly new device concepts for III–V nanostructure based photonic devices.

ASSOCIATED CONTENT

ⓢ Supporting Information. In MacEtch, the metal catalyst acts as the cathode and the semiconductor acts as the anode. Table lists relevant half reactions involving chemical species used for etching in this article as well as possible products and participating reactants in the overall reaction. This material is available free of charge via the Internet at http://pubs.acs.org.

AUTHOR INFORMATION

Corresponding Author
*E-mail: Xiuling@illinois.edu.

ACKNOWLEDGMENT

REFERENCES

(1) Yu, K.; Chen, J. *Nanoscale Res. Lett.* **2009**, *4*, 1–10.
(2) Yan, R.; Gargas, D.; Yang, P. *Nat. Photonics* **2009**, *3*, 569–576.
(3) Min-An, T.; Peichen, Y.; Chao, C. L.; Chiu, C. H.; Kuo, H. C.; Lin, S. H.; Huang, J. J.; Lu, T. C.; Wang, S. C. *IEEE Photonics Technol. Lett.* **2009**, *21*, 257–259.
(4) Bryllert, T.; Wernersson, L. E.; Froberg, L. E.; Samuelson, L. *IEEE Electron Device Lett.* **2006**, *27*, 323–325.
(5) Hochbaum, A. I.; Chen, R.; Delgado, R. D.; Liang, W.; Garnett, E. C.; Najarian, M.; Majumdar, A.; Yang, P. *Nature* **2008**, *451*, 163–167.
(6) Martinez, L. J.; Prieto, I.; Alen, B.; Postigo, P. A. *J. Vac. Sci. Technol., B: Microelectron. Nanometer Struct.—Process., Meas., Phenom.* **2009**, *27*, 1801–1804.
(7) Ping, A.; Chen, Q.; Yang, J.; Khan, M.; Adesida, I. *J. Electron. Mater.* **1998**, *27*, 261–265.
(8) Lishan, D. G.; Wong, H. F.; Green, D. L.; Hu, E. L.; Merz, J. L.; Kirillov, D. *J. Vac. Sci. Technol., B: Microelectron. Nanometer Struct.—Process., Meas., Phenom.* **1989**, *7*, 556–560.
(9) Huang, Z.; Geyer, N.; Werner, P.; de Boor, J.; Gösele, U. *Adv. Mater.* **2011**, *23*, 285–308.
(10) Li, X.; Bohn, P. W. *Appl. Phys. Lett.* **2000**, *77*, 2572–2574.
(11) Peng, K. Q.; Hu, J. J.; Yan, Y. J.; Wu, Y.; Fang, H.; Xu, Y.; Lee, S. T.; Zhu, J. *Adv. Funct. Mater.* **2006**, *16*, 387–394.
(12) Chartier, C.; Bastide, S.; Lévy-Clément, C. *Electrochim. Acta* **2008**, *53*, 5509–5516.
(13) Chen, H.; Wang, H.; Zhang, X.-H.; Lee, C.-S.; Lee, S.-T. *Nano Lett.* **2010**, *10*, 864–868.
(14) Chern, W.; Hsu, K.; Chun, I. S.; de Azeredo, B. P.; Ahmed, N.; Kim, K. H.; Zuo, J. M.; Fang, N.; Ferreira, P.; Li, X. L. *Nano Lett.* **2010**, *10*, 1582–1588.
(15) Chun, I. S.; Chow, E. K.; Li, X. *Appl. Phys. Lett.* **2008**, *92*, 191113.
(16) Rykaczewski, K.; Hildreth, O. J.; Kulkarni, D.; Henry, M. R.; Kim, S.-K.; Wong, C. P.; Tsukruk, V. V.; Fedorov, A. G. *ACS Appl. Mater. Interfaces* **2010**, *2*, 969–973.
(17) Huang, Z.; Fang, H.; Zhu, J. *Adv. Mater.* **2007**, *19*, 744–748.
(18) Asoh, H.; Yokoyama, T.; Ono, S. *Jpn. J. Appl. Phys.* **2010**, 49.
(19) Yasukawa, Y.; Asoh, H.; Ono, S. *J. Electrochem. Soc.* **2009**, *156*, H777–H781.
(20) Yasukawa, Y. *Electrochem. Commun.* **2008**, *10*, 757–60.
(21) Barycka, I.; Zubel, I. *J. Mater. Sci.* **1987**, *22*, 1299–1304.
(22) Rogers, J. A.; Nuzzo, R. G. *Mater. Today* **2005**, *8*, 50–56.
(23) Kim, J.; Kim, Y. H.; Choi, S.-H.; Lee, W. *ACS Nano* **2011**, *5*, 5242–5248.
(24) CRC Handbook of Chemistry and Physics, 92nd ed.: Haynes, W. M., Ed.; CRC Press: Boca Raton, FL, 2011.